

The Myc-evoked DNA damage response accounts for treatment resistance in primary lymphomas in vivo

Maurice Reimann,¹ Christoph Loddenkemper,² Cornelia Rudolph,³ Ines Schildhauer,¹ Bianca Teichmann,¹ Harald Stein,² Brigitte Schlegelberger,³ Bernd Dörken,^{1,4} and Clemens A. Schmitt^{1,4}

¹Charité–Humboldt University, Campus Virchow, Department of Hematology/Oncology, Berlin; ²Charité–Humboldt University, Campus Benjamin Franklin, Department of Pathology, Berlin; ³Institute of Cell and Molecular Pathology, Hannover Medical School, Hannover; and ⁴Max-Delbrück-Center for Molecular Medicine, Berlin, Germany

In addition to the ARF/p53 pathway, the DNA damage response (DDR) has been recognized as another oncogene-provoked anticancer barrier in early human tumorigenesis leading to apoptosis or cellular senescence. DDR mutations may promote tumor formation, but their impact on treatment outcome remains unclear. In this study, we generated ataxia telangiectasia mutated (Atm)-proficient and -deficient B-cell lymphomas in *Eμ-myc* transgenic mice to examine the role of DDR defects in lymphomagenesis and treatment sensitivity.

***Atm* inactivation accelerated development of lymphomas, and their DNA damage checkpoint defects were virtually indistinguishable from those observed in *Atm*^{+/+}-derived lymphomas that spontaneously inactivated the proapoptotic *Atm*/p53 cascade in response to Myc-evoked reactive oxygen species (ROS). Importantly, acquisition of DDR defects, but not selection against the ARF pathway, could be prevented by life-long exposure to the ROS scavenger N-acetylcysteine (NAC) in vivo. Following anticancer therapy, DDR-compromised**

lymphomas displayed apoptotic but, surprisingly, no senescence defects and achieved a much poorer long-term outcome when compared with DDR-competent lymphomas treated in vivo. Hence, *Atm* eliminates preneoplastic lesions by converting oncogenic signaling into apoptosis, and selection against an *Atm*-dependent response promotes formation of lymphomas with predetermined treatment insensitivity. (Blood. 2007;110:2996-3004)

© 2007 by The American Society of Hematology

Introduction

Cancer development is a process against which normal cells appear to be well protected.¹ As an early cellular barrier against imminent transformation, normal cells monitor latent oncogenic signals, which may result in activation of the ARF/p53 axis as an antiproliferative constraint, ultimately leading to apoptosis or cellular senescence.² In turn, genetic defects in these oncogene-induced fail-safe programs are prerequisites for malignant conversion and thus are selected for in manifest malignancies.³⁻⁵

In addition, oncogene-related cellular stress enacting a DNA damage response (DDR) has been proposed as an ARF-independent constraint to limit aberrant cell division in early tumorigenesis via induction of apoptosis or senescence.⁶⁻¹⁰ Indeed, prototypic oncogenes such as Myc and Ras have been reported to cause DNA damage, possibly via the production of reactive oxygen species (ROS)^{11,12} or by generating aberrant DNA replication intermediates.^{13,14} Conversely, inherited DDR defects as known from ataxia telangiectasia (A-T),¹⁵ the Nijmegen breakage syndrome (Nbs),¹⁶ or the Li-Fraumeni syndrome (affecting *Chk2* or *p53*)^{17,18} predispose to cancer, presumably by facilitating mutagenic activation and permitting transforming action of mitogenic oncogenes.¹⁹ Immunohistochemical studies on epithelial tumor specimens of various developmental stages driven by unspecified oncogenic moieties found hyperproliferative precursor lesions to display activated components of the Atr/Nbs1/Chk1 and the *Atm*/Chk2/p53 DDR

cascades, whereas this activation was lost in more advanced neoplastic lesions, thereby suggesting a tumor-suppressive role of the DDR.^{7,8}

Atm, a key component of the DDR and identified as the gene that is mutated in A-T,¹⁵ encodes a phosphatidylinositol-3-kinase-like protein kinase that phosphorylates numerous substrates upon DNA damage.²⁰ Genotoxic stress or related cellular insults initiate, at least in part via the ataxia telangiectasia-mutated (*Atm*)-interacting protein phosphatase 5 (PP5), intermolecular autophosphorylation at serine 1981 (ie, serine 1987 in mice) and, together with other molecular changes, lead to *Atm* activation.²¹⁻²³ *Atm* augments the growth-suppressive potential of ARF in focus formation assays by transducing and converting oncogene-derived signals into p53 activation independent of ARF.^{24,25} A-T patients with biallelic *Atm* inactivation are predisposed to various malignancies mostly of lymphoid origin and produce massive damage in their normal tissue when exposed to radiation therapy. Whereas the radiohypersensitivity of A-T cells, typically tested in fibroblasts or normal lymphocytes derived from A-T patients, is reflected by overt chromosomal damage and uninterrupted DNA synthesis, there is no clear indication of a primary apoptotic defect in these cells.^{26,27} Many hematologic malignancies have selected for *Atm* mutations during tumor progression and therapy, although findings

Submitted February 21, 2007; accepted May 29, 2007. Prepublished online as *Blood* First Edition paper, June 11, 2007; DOI 10.1182/blood-2007-02-075614.

The online version of this article contains a data supplement.

Presented in abstract form at the 48th annual meeting of the American Society

of Hematology, Orlando, FL, December 12, 2006.

The publication costs of this article were defrayed in part by page charge payment. Therefore, and solely to indicate this fact, this article is hereby marked "advertisement" in accordance with 18 USC section 1734.

© 2007 by The American Society of Hematology

regarding the relationship between *Atm* inactivation and clinical outcome remain controversial.^{28,29}

A number of studies indicated a link between oncogenic *Myc* activation with *Atm* inactivation during tumorigenesis in different entities, including human B-cell lymphomagenesis.³⁰ In mice, extra copies of chromosome 15, to where the *c-myc* gene maps, were found in *Atm*^{-/-} thymic lymphomas,³¹ and recent studies demonstrated the collaboration of *Atm* loss and *Myc* activation in murine models of skin and lymphoid malignancies.^{32,33} Despite the increasing evidence for DDR impairment following oncogenic activation, the underlying mechanism by which oncogenes provoke spontaneous DDR defects and their subsequent clinical implications for treatment outcome remains elusive.

In this study, we used the *Eμ-myc* transgenic mouse model to comprehensively analyze the functional implications of genetically defined—as compared with sporadic—DDR defects on tumor biology and, in particular, treatment sensitivity in a large series of primary B-cell lymphomas. Our findings dissect *Myc*-driven activation of the DDR as an ROS-initiated and *Atm*-governed proapoptotic process that is selected against during lymphoma formation and demonstrate the profound impact of predefined or spontaneously acquired DDR lesions on the efficacy and long-term outcome to anticancer treatments in vitro and in vivo. Furthermore, we explore in vivo how pharmacologic intervention might preserve an intact DDR to subsequently improve the efficacy of DNA-damaging chemotherapy.

Materials and methods

Mice, cells, and drug treatments

All animal protocols used in this study were approved by the governmental review board (Landesamt für Gesundheit und Soziales, Berlin, Germany). Lymphomas harboring loss-of-function lesions were generated by intercrossing *Eμ-myc* transgenic mice³⁴ with mice harboring targeted deletions at the *Atm*,³⁵ *p53*,³⁶ *ARF*,³⁷ or *Nbs1*³⁸ locus (all genotypes in BL/6 background). Monitoring of lymph nodes, processing and fixation of tissues, isolation of lymphoma cells or splenic B-lymphocytes (purified via immunobead separation [Miltenyi Biotec, Bergisch Gladbach, Germany]), and short-term cultivation and transplantation of lymphoma cells were performed as described.^{5,39} Preneoplastic samples are derived from mice of approximately 25 days of age with no signs of lymph node or spleen enlargement and absence of leukemia. For in vivo treatments, tumor-bearing mice received a single dose of either 4 Gy γ -irradiation or 300 mg/kg body weight of cyclophosphamide (CTX) intraperitoneally.⁴ N-acetylcysteine (NAC; Hexal, Holzkirchen, Germany) was applied as a 0.5% wt/vol supplementation to the drinking water starting at a midembryonic stage and continued for life. For in vitro treatments, cells were exposed to 0.2 μ g/mL (unless otherwise stated) adriamycin (ADR) (Sigma-Aldrich, Taufkirchen, Germany) for various periods of time as indicated. Lymphocytes were stimulated with 50 μ g/mL lipopolysaccharide (LPS) from *Escherichia coli* (Fluka). NAC-pretreated lymphoma cells were exposed to DNA-damaging agents after 3 days of NAC-free maintenance. Statistical comparison of Kaplan-Meier curves is based on the log-rank test; the unpaired *t* test was applied for comparisons of means and standard deviations (SD; asterisk denotes significance as *P* < .05). In all figures, error bars shown denote the SD.

Retroviral gene transfer, siRNA-mediated knockdown, and inducible gene expression

Retroviral gene transfer using MSCV-bcl2-IRES-GFP has been described.³⁹ Knockdown of specific transcripts was achieved by stable introduction of retroviral siRNA cloned into the pSuper.Retro system (Oligo Engine, Seattle, WA; [Atm-siRNA: 5'-GTCTAGCACTCAATGATCT-3'; PP5-siRNA: 5'-GACAGAGAAGATTACAGTG-3']). MycER^{TAM} cells, generated by infecting mouse embryo fibroblasts (MycER^{TAM}-MEFs)

or (ARF-deficient) NIH3T3 fibroblasts (MycER^{TAM}-3T3) with the MSCV-MycER^{TAM}-blasticidin retrovirus, were treated with 1 μ M 4-hydroxytamoxifen (OHT; Sigma-Aldrich) or the equivalent volumes of the ethanol-based solvent.

Analysis of cellular integrity, DNA strand breaks, and metabolic condition

Cellular viability and DNA content were assessed by 7-amino-actinomycin D (Sigma-Aldrich) dye exclusion or propidium iodide-based DNA staining measured by flow cytometry and quantified using ModFit LT 2.0 Software (Verity Software House, Topsham, ME).⁵ Cellular senescence was detected by staining for the senescence-associated β -galactosidase activity in cytospin preparations at pH 5.5 as described.⁵ ROS levels were measured by flow cytometry in freshly isolated cells after incubation in 10 μ M 2'-7'-dichlorodihydrofluorescein diacetate (Gibco, Karlsruhe, Germany). Oxidatively modified DNA was quantified by the formamidopyrimidine-DNA glycosylase (Fpg)-COMET assay.⁴⁰ Briefly, cells were embedded in low-melting-point agarose, lysed, and exposed to Fpg (New England Biolabs, Frankfurt am Main, Germany). After gel electrophoresis and DAPI staining, mean tail moments of randomly chosen comets were quantified as the relative increment following Fpg treatment using the CometScore (TriTek, Summerduck, VA) software V1.5 for analysis. γ -H2AX foci, detected by immunofluorescence, were quantified by counting at least 25 cells per sample. Apoptosis-related DNA fragmentation was visualized using a fluorescence-based terminal deoxy-nucleotidyl transferase dUTP nick end labeling (TUNEL) assay (Roche Diagnostics, Mannheim, Germany) with DAPI as a counterstain in some experiments. Cells were mounted using VECTASHIELD (Vector Laboratories, Burlingame, CA) mounting medium for fluorescence. Images of cells were captured by the Axioplan fluorescence microscope with Plan-Neofluar objectives (100 \times /1.30 NA oil or 40 \times /0.75 NA) (Carl Zeiss, Jena, Germany) attached to a SPOT RT camera model 2.3.1 and imported into SpotAdvanced v3.5 software (Diagnostic Instruments, Sterling Heights, MI).

Analysis of chromosomal aberrations, V(D)J recombination, and genomic mutations

Chromosomal aberrations in primary lymphomas were assessed in stained metaphase spreads by fluorescence microscopy and spectral karyotyping.⁵ To detect V(D)J recombinations, *IgH* loci were amplified in a first genomic polymerase chain reaction (PCR) using 9 VH- or DH-specific and 1 JH-specific primers, followed by a second-round PCR containing a single VH or DH primer together with a nested JH primer.⁴¹ A productive PCR indicates an accomplished rearrangement. Primer sequences are available upon request. *p53* mutations within exons 5 to 8 were assessed by reverse transcriptase (RT)-PCR-based sequencing and homozygous gross deletions at the *INK4a/ARF* locus by a genomic multiplex PCR.⁴ Using primers spanning exon 1 β to exon 2, RT-PCR-based expression analysis of ARF transcripts (and TATA-box binding protein [TBP] as an internal control) was carried out as described.⁵

Protein analysis by immunophenotyping, immunostaining, and immunoblot

Immunophenotyping by flow cytometry as well as antigen detection by immunohistochemistry and by immunofluorescence of permeabilized cytospin preparations were carried out as described.⁵ Whole-cell extracts for immunoblotting were prepared by lysing cells in 200 mM NaCl, 50 mM Tris (pH 8.0), 5 mM EDTA, 1% Triton X-100, 10% glycerol, 1 mM sodium orthovanadate, 2 mM dithiothreitol (DTT), 1.5 μ g/mL aprotinin, 0.3 mg/mL pepabloc, and 6 μ g/mL leupeptin. Primary antibodies raised against Atm (GeneTex, Hiddenhausen, Germany), Atm-P-S1981 (ie, Atm-P-S1987 in mice; Cell Signaling Technology, Boston, MA), Atr-P-S428 (ie, Atr-P-S431 in mice, a putative site of Atr activation; Cell Signaling Technology), Atr (Santa Cruz Biotechnology, Santa Cruz, CA), ARF (Abcam, Cambridge, United Kingdom), Bcl2 (BD Pharmingen, Franklin Lakes, NJ), c-Myc (Santa Cruz Biotechnology), p53 (Novocastra, Newcastle, United Kingdom), p53-P-S18 (Cell Signaling Technology), PP5 (BD Pharmingen),

α -tubulin (Sigma-Aldrich), γ -H2AX (Upstate, Temecula, CA), Ki67 (Dako, Hamburg, Germany), caspase-3 (Cell Signaling Technology), cleaved caspase-3/Asp175 (Cell Signaling Technology), CD45/B220 (BD Pharmingen), CD43 (BD Pharmingen), and CD90.2/Thy1.2 (BD Pharmingen) were used, if required, with corresponding peroxidase- and fluorescence-conjugated secondary antibodies (GE Healthcare, München, Germany; Molecular Probes, Karlsruhe, Germany; Santa Cruz Biotechnology), and visualized as described.^{5,39}

Results

Myc provokes an Atm-dependent DDR leading to apoptosis in preneoplastic B cells in vivo

NIH3T3 fibroblasts stably expressing an OHT-inducible *c-Myc*/estrogen receptor fusion protein (MycER^{TAM}-3T3) confirmed that acute induction of Myc—like exposure to the DNA-damaging anticancer agent adriamycin (ADR)—elicits a PP5/Atm-dependent DDR leading to phosphorylation of p53 at serine 18 (p53-P-S18) in vitro (Figure S1, available on the *Blood* website; see the Supplemental Materials link at the top of the online article). To examine the role of the Atm-governed DDR in response to oncogenic Myc signaling in vivo, B-cell lymphoma-prone *E μ -myc* transgenic mice heterozygous for germ-line deletions at the *Atm* locus (*Atm*^{+/-}) were intercrossed with *Atm*^{+/-} mice.^{34,35} Immunoblot analysis of

nontransgenic compared with preneoplastic B lymphocytes constitutively expressing Myc unveiled a strong activation of DDR components such as Atm-P-S1987 and p53-P-S18 in response to Myc that strictly depend on Atm (Figure 1A). Importantly, proapoptotic cleavage of caspase-3 was detectable in Atm-proficient *E μ -myc* transgenic B lymphocytes but not in Atm-deficient cells or B cells lacking constitutive Myc signaling, indicating that Atm is required for Myc-provoked apoptosis in vivo. Accordingly, when the steady state amount of spontaneous apoptosis was determined as a fraction of DNA-fragmented TUNEL-positive cells, much more apoptosis was detected in the *E μ -myc* transgenic compared with the nontransgenic population, whereby the amount of Myc-induced cell death was significantly reduced in the absence of Atm ($P = .037$; Figure 1B). Thus, the activated Atm/p53 signature in the oncogene-exposed murine B-cell compartment recapitulates the occurrence of a proapoptotic DDR as previously detected in early hyperproliferative stages of human (pre)carcinomatous tissue samples.^{7,8}

Atm inactivation collaborates with constitutive Myc expression in lymphomagenesis

Myc-driven lymphomas arising in *Atm*^{+/+} mice, hereafter referred to as controls, became detectable as a palpable lymphadenopathy with associated leukemia at a median age of 101 days, whereas *Atm*^{-/-} mice displayed lymphomas with a median onset of 50 days, significantly earlier ($P < .001$) (Figure 1C). Lymphoma development in *Atm*^{+/-} mice was virtually indistinguishable from that observed in the *Atm*^{+/+} group. Notably, all *E μ -myc*-initiated tumors were B220⁺ and Thy1.2⁻ (data not shown), indicating that Atm-deficient *E μ -myc* mice succumbed to B-cell lymphomas before thymic T-cell lymphomas that typically arise in nontransgenic *Atm*^{-/-} mice could form and disseminate.³⁵ Manifest lymphomas displayed reduced amounts of spontaneous apoptosis in the absence of Atm, as seen during tumor development for preneoplastic stages, while the proliferation rate appeared to be unaffected by the Atm status, indicating that the Atm-governed S-phase checkpoint is not challenged or became dysfunctional in constitutive Myc-driven lymphomagenesis (Figure S2A,B). Furthermore, *Atm*^{-/-} lymphomas grew more aggressively than controls, as reflected by their dissemination into nonlymphoid organs such as lung and pancreas (Figure 1D).

Both control and *Atm*^{-/-} lymphomas accomplished clonal V(D)J recombination and progressed to a more mature, CD43⁻ B-cell state, indicating that differentiation was not blocked in the absence of Atm (Figure S2C and data not shown). Spectral karyotyping of *Atm*^{-/-} samples confirmed no signs of gross aneuploidy but revealed a higher frequency of nonrecurrent translocations (6 of 7 *Atm*^{-/-} compared with 2 of 7 control samples tested; Figure S2D-E), highlighting the role of Atm in proper DNA double-strand break repair.

Hence, Atm resides in a proapoptotic signaling pathway that is activated during Myc-driven lymphomagenesis to counter malignant transformation, and inactivation of *Atm* alleles promotes development of apoptotically compromised lymphomas in a nonhaploinsufficient fashion.

The Atm/p53 and ARF/p53 axes cooperate as proapoptotic growth restraints in Myc-driven lymphomagenesis

Inactivation of ARF, the Myc-inducible tumor suppressor controlling p53 protein levels via interaction with Mdm2,^{42,43} has been

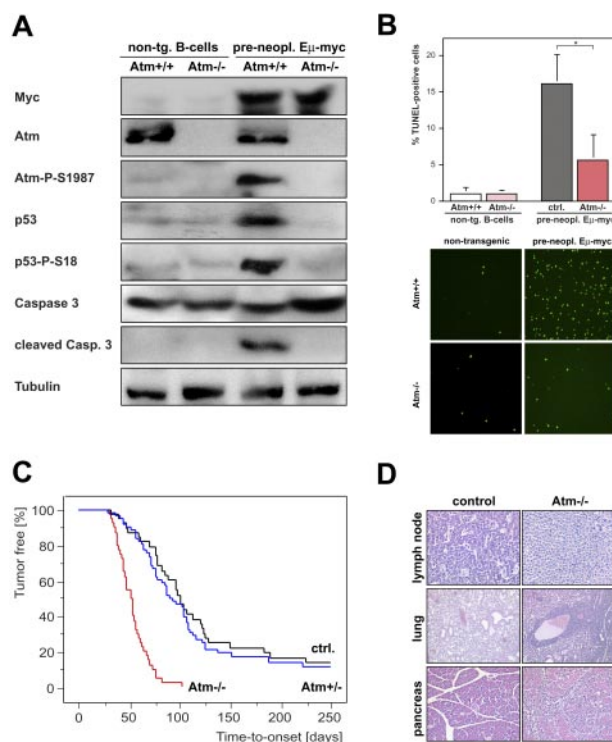


Figure 1. Myc challenges tumor-suppressive Atm signaling in the B-cell compartment in vivo. (A) Immunoblot analysis of the Atm-governed DDR signature consisting of Atm, Atm-P-S1987, p53, p53-P-S18, and caspase-3 with its proapoptotic cleavage product in lysates of immunobead-selected Atm-proficient and -deficient nontransgenic and preneoplastic *E μ -myc* transgenic B cells with tubulin as a loading control. (B) Spontaneous apoptosis of *Atm*^{+/+} and *Atm*^{-/-} nontransgenic and preneoplastic *E μ -myc* transgenic B cells in cytospin preparations ($n = 4$) quantified by fluorescence-based TUNEL staining. Data are expressed as mean plus or minus SD; * $P < .05$. (C) Lymphoma incidence in *E μ -myc* transgenic mice in an *Atm*^{+/+} (control [ctrl]; $n = 44$; black), *Atm*^{+/-} ($n = 74$; blue), and *Atm*^{-/-} ($n = 44$; red) background. (D) Histopathological presentations of *E μ -myc* control and *Atm*^{-/-} lymphomas. Representative photomicrographs of hematoxylin and eosin-stained tissue sections of the indicated organs obtained at manifestation. Original magnification, $\times 200$.

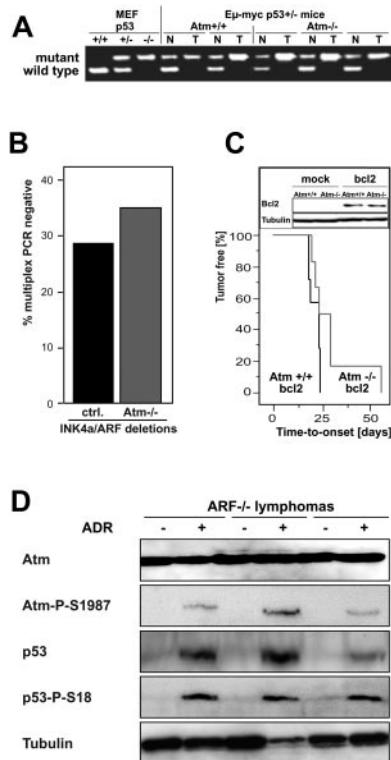


Figure 2. The ARF/p53 and Atm/53 axes cooperate as proapoptotic growth restraints in Myc-driven tumorigenesis. (A) Genomic *p53* status by allele-specific PCR in primary *Eμ-myc* lymphomas that formed in an *Atm*^{+/+}; *p53*^{+/-} or an *Atm*^{-/-}; *p53*^{+/-} background (normal tissue [N] compared with the matched tumor tissue [T] for every given animal); MEFs of the indicated *p53* genotypes as controls. (B) Frequency of homozygous *INK4a/ARF* deletions that cancel ARF expression in control (ctrl) and *Atm*^{-/-} lymphomas detected by multiplex PCR of exon 1β and 2 (control, 8 of 19 cases; *Atm*^{-/-}, 5 of 14 cases tested). (C) Lymphoma incidence in lethally irradiated recipient mice of retrovirally *bcl2*-infected *Eμ-myc* transgenic *Atm*^{+/+} and (control [ctrl]; n = 7; black) *Atm*^{-/-} (n = 6; red) hematopoietic stem cells. Note the very early onset due to the *Bcl2* moiety (see Schmitt et al⁴⁵ for comparison with onset data upon mock infection). Immunoblot analysis testing for *Bcl2* expression in lymphomas generated from transplanted *bcl2*- or mock-infected *Eμ-myc* hematopoietic stem cells (representative samples shown). (D) Immunoblot analysis of DDR components in *ARF*^{-/-} *Eμ-myc* lymphoma cell lysates exposed to adriamycin (ADR; 0.2 μg/mL for 5 hours) in vitro or left untreated.

demonstrated to accelerate lymphomagenesis in *Eμ-myc* transgenic mice.^{3,44} To genetically explore whether an *Atm*-dependent apoptotic defect would alleviate the selective pressure against the ARF/p53 antioncogenic restraint in *Myc*-driven lymphomagenesis, we generated *Eμ-myc* transgenic *p53*^{+/-} mice with and without *Atm* genes. As reported for the *Atm*^{+/+} condition,⁴ *Eμ-myc* lymphomas forming in *Atm*^{-/-}; *p53*^{+/-} mice still deleted the remaining *p53* wild-type allele (Figure 2A). Accordingly, similar frequencies of spontaneous homozygous deletions of the *INK4a/ARF* exons 1β or 2 that cancel ARF protein expression were found in control and *Atm*^{-/-} lymphomas (Figure 2B), indicating that *Atm* loss cannot alleviate the pressure to inactivate the *Myc*-induced ARF/p53 axis. Next, we asked whether disruption of apoptosis downstream of *p53* would neutralize the accelerating impact of *Atm* loss on *Myc*-driven lymphomagenesis. Indeed, retroviral transfer of the antiapoptotic *bcl2* gene into *Eμ-myc* transgenic hematopoietic stem cells—sufficient to protect from *p53* inactivation in *Myc*-driven lymphomagenesis⁴⁵—produced lymphomas in recipient mice resulting in an onset that was no longer affected by the *Atm* gene status (Figure 2C). Furthermore, *Eμ-myc* transgenic lymphomas lacking both *ARF* alleles typically expressed low levels of wild-type *p53* but retained an inducible, *Atm*-dependent DDR

that became evident after exposure to ADR (Figure 2D).³ Hence, the *Atm*-mediated antioncogenic response complements ARF signaling to the common downstream effector *p53* to counter oncogenic transformation via execution of apoptosis.

A subset of manifest Myc lymphomas displays functional defects in the *Atm*-governed DDR

Because the *Myc*-initiated DDR signature is present in preneoplastic B cells (Figure 1A), we hypothesized that full-blown malignancies might have selected for *Atm*-related DDR defects during lymphomagenesis. We therefore scanned primary control lymphomas for the presence or absence of activated DDR components by immunoblot analysis. Beside detectable basal levels of phosphorylation-activated *Atm* (ie, *Atm*-P-S1987) in some cases, 6 of 12 control lymphomas tested exhibited considerable amounts of *p53*-P-S18, whereas these phospho-proteins were not detectable in normal B cells (Figure 3A) and *Atm*^{-/-} lymphomas (Figure 3B). No activated DDR mediators could be visualized in any of the remaining control lymphomas tested despite comparable *Myc* expression levels,⁴⁶ indicating either lack of basal activation or structural inactivation of this pathway in about half of the samples.

Therefore, we tested whether stimulation by exogenous DNA damage may either result in a detectable DDR or might unmask checkpoint defects such as impaired apoptotic activation or “drug damage-resistant cell cycle progression into S phase” reminiscent

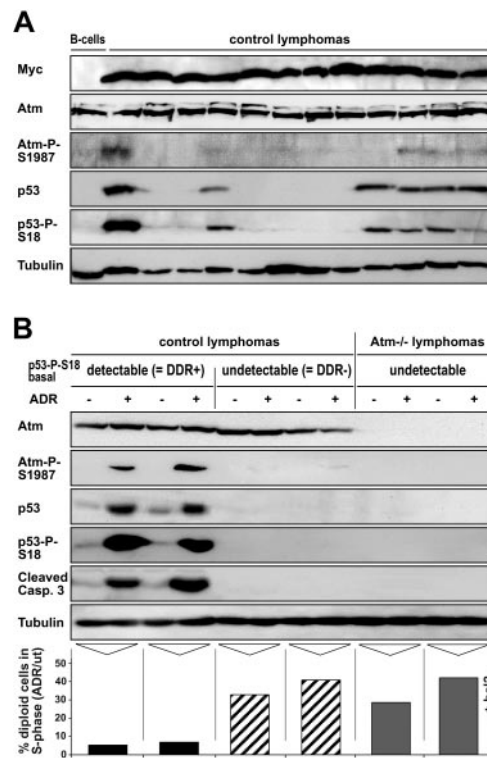


Figure 3. DDR-compromised Myc lymphomas share checkpoint defects with *Atm*-deficient lymphomas. (A) Immunoblot analysis of *Myc*, *Atm*, *Atm*-P-S1987, *p53*, *p53*-P-S18, and tubulin as a loading control in immunobead-isolated normal B cells and 12 randomly selected control lymphomas. (B) Immunoblot analysis of *Atm*, *Atm*-P-S1987, *p53*, *p53*-P-S18, cleaved caspase-3, and tubulin as a loading control in *Atm*^{-/-} and representative control lymphomas with detectable versus undetectable basal *p53*-P-S18 levels (compare with panel A); basal (-) and induced (+) levels 5 hours after ADR in vitro, aligned with the relative (ADR/no ADR [ut indicates untreated]) S-phase fraction of the same lymphoma samples, now stably expressing *Bcl2*, 48 hours after ADR or left untreated. Shown are representative examples of the entirety of lymphomas presented in panel A.

of the “radioresistant DNA synthesis” checkpoint defect known from *Atm*^{-/-} cells.⁴⁷ Control lymphomas that formed with detectable basal p53-P-S18 levels consistently produced strongly induced p53-P-S18 levels accompanied by high amounts of apoptosis-related cleaved caspase-3 after exposure to ADR, a signature that was entirely absent in control lymphomas with undetectable basal p53-P-S18 levels and in *Atm*^{-/-} lymphomas prior to and after ADR (Figure 3B top). Thus, control lymphomas with detectable and ADR-inducible p53-P-S18 levels were considered DDR competent (“DDR+,” 6 of 12 cases tested), whereas those not producing any p53-P-S18 band (despite wild-type *p53* genes by sequencing analysis [of 12 control and *Atm*^{-/-} lymphomas each]; data not shown) formed the DDR-impaired (“DDR-,” 6 of 12 cases tested) group. Importantly, when the same individual lymphoma cell populations were exposed to ADR after stable infection with a *bcl2* retrovirus to block apoptosis, *Atm*^{-/-} and DDR- control lymphomas but not DDR+ lymphomas exhibited considerable DNA synthesis activity as indicated by cells in S phase (Figure 3B bottom). Hence, reduced basal levels of DDR components selected for in control lymphomas reflect genetic lesions that produce a drug damage-resistant and apoptotically compromised phenotype virtually indistinguishable from the checkpoint defects detectable in *Atm*^{-/-} lymphomas.

Lymphomas developing under ROS scavengers preserve an intact DDR machinery

Given our observation that Myc signaling—like treatment with a DNA-damaging compound—provokes PP5/Atm-dependent p53 activation (Figure S1), we aimed to assess marks of DNA damage in Myc-driven lymphomas with different *Atm* background. ROS—a potential cause of DNA lesions that have been associated with Myc activation *in vitro*¹²—were detectable at significantly increased levels in *Eμ-myc* lymphoma cells compared with nontransgenic *Atm*^{+/+} and *Atm*^{-/-} B cells (Figure 4A). Consequently, quantification of DNA damage as a result of oxidative stress using the Fpg-COMET assay unveiled higher numbers of DNA strand breaks

in Myc-driven lymphomas compared with nontransgenic B cells irrespective of their *Atm* status (Figure 4B). Phosphorylation of the histone H2A variant, H2AX, at serine 139 is known as an early, *Atm*-mediated response to DNA double-strand breaks, resulting in γ -H2AX foci at the sites of DNA damage.⁴⁸ The number of γ -H2AX foci was found markedly increased under constitutive Myc expression compared with nontransgenic B cells and appeared to be independent of *Atm* (Figure 4C). Most γ -H2AX foci measured in manifest *Eμ-myc* lymphomas reflect sites of endogenous DNA damage rather than marks at apoptotic strand breaks, because similar levels of γ -H2AX foci were also detected in *Atm*^{-/-} and control lymphomas stably overexpressing the antiapoptotic Bcl2 protein. Because γ -H2AX foci may form in an *Atm*-independent fashion via substituting action of the related Atr (ataxia-telangiectasia Rad3-related) kinase,⁴⁹ it is conceivable that comparable steady state levels of γ -H2AX foci in control versus *Atm*^{-/-} lymphoma cells may result from the extended persistence of unresolved DNA strand breaks in the absence of proper *Atm* function. Indeed, immunoblot analysis confirmed the presence of serine 431-phospho-activated Atr (Atr-P-S431) in *Atm*^{-/-} and, less profoundly, in control lymphomas but not in nontransgenic B cells (Figure 4D). Importantly, LPS-enforced proliferation of nontransgenic primary B cells to an extent comparable with Myc-driven lymphoma cell proliferation produced a much smaller increase of ROS levels (1.5-fold versus about 5-fold) and was not associated with enhanced numbers of γ -H2AX foci (Figure 4E). Thus, the profound increase in marks of DNA damage in Myc-driven cells with or without *Atm* is predominantly linked to genotoxic but not to hyperproliferative signaling emanating from the oncogene.

These findings indicated that Myc-evoked oxidative stress acts as the upstream signal that instates the selective pressure against a functional DDR machinery as observed in a subset of control lymphomas (Figure 3A). Therefore, we examined lymphoma development when oxidative stress is pharmacologically blunted by the ROS scavenger NAC, which prevents DNA damage and protects cells from a subsequent PP5/Atm-dependent DDR elicited

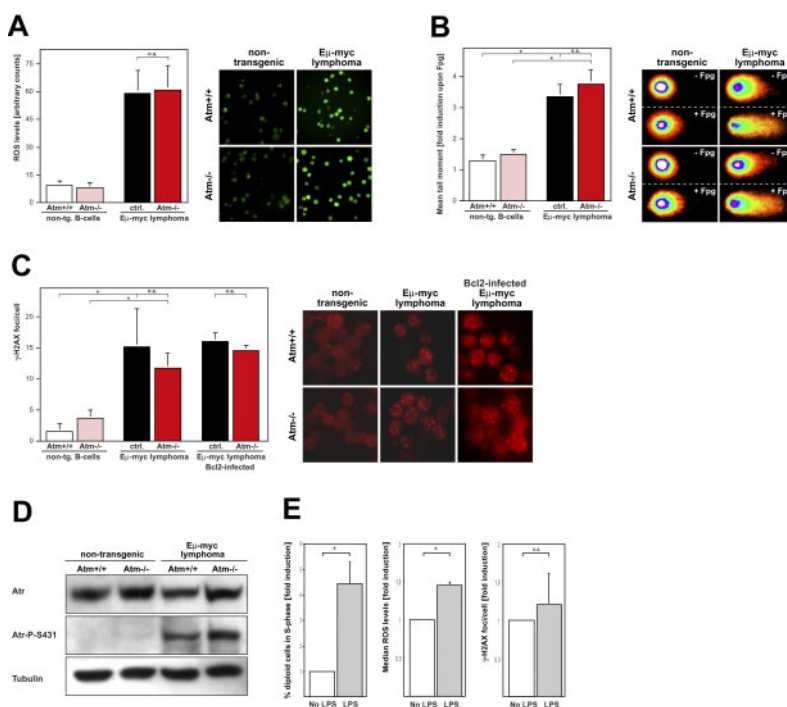


Figure 4. Myc induces DNA damage via ROS *in vivo*. Comparison of freshly isolated *Eμ-myc* lymphoma cells and immunobead-selected nontransgenic B cells derived from an *Atm*^{+/+} or an *Atm*^{-/-} background ($n = 4$ individual samples per genotype). (A) 2'-7'-Dichlorodihydrofluorescein diacetate–based flow cytometric analysis of cellular ROS levels (left); representative example visualized by fluorescence microscopy (right). Original magnification, $\times 200$. (B) Oxidative DNA damage measured as the relative induction of mean tail moments in the COMET assay prior to and after treatment with Fpg; quantification (left); representative examples of comets (right). (C) γ -H2AX foci per cell in cytospin preparations; same cell populations stably expressing Bcl2 to block apoptosis in the right panel; quantification (left) and representative examples (right). (D) Immunoblot analysis of total Atr, Atr-P-S431, and tubulin as a loading control in nontransgenic B lymphocytes as compared with representative control and *Atm*^{-/-} *Eμ-myc* lymphomas. (E) Proliferation (left, cells with S-phase DNA content), ROS induction (middle, as in panel A), and γ -H2AX foci (right, as in panel C) in primary nontransgenic B cells displayed as relative values at 48 hours after LPS stimulation (50 μ g/mL) compared with no LPS.

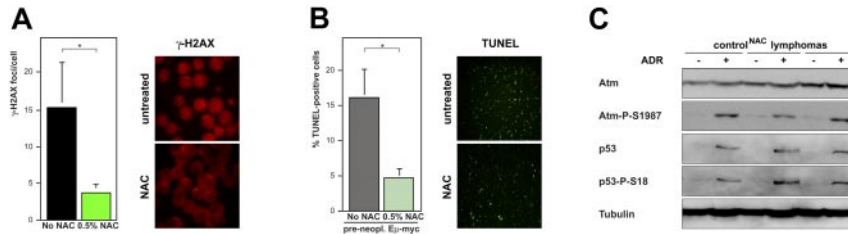


Figure 5. Blunting Myc-evoked ROS preserves a latent DDR machinery in vivo. (A) DNA damage sites visualized as γ -H2AX foci in cytospin preparations of *E μ -myc* control lymphomas that formed with and without lifelong exposure to NAC; quantification (left) and representative examples (right). Original magnification, $\times 1000$. (B) Spontaneous apoptosis by fluorescence-based TUNEL staining in cytospin preparations of preneoplastic *E μ -myc* transgenic B cells (exposure to NAC as in panel A). Original magnification, $\times 200$. (C) Immunoblot analysis of Atm, Atm-P-S1987, p53, p53-P-S18, and tubulin as a loading control in NAC-protected control lymphomas; basal (–) and induced (+) levels 5 hours after ADR in vitro. All quantitative data are mean \pm SD; * $P < .05$; NS indicates not significant.

by Myc in established cell lines in vitro (Figure S3A).^{12,50} *E μ -myc* transgenic mice were continuously exposed to NAC-supplemented drinking water starting at a midembryonic age. Importantly, when γ -H2AX foci were quantified in NAC-pretreated versus untreated lymphomas at manifestation, significantly less foci were found in NAC-protected control lymphomas ($P = .016$; Figure 5A), indicating that Myc-originated signals otherwise leading to DNA damage were blunted by the ROS scavenger. Consequently, lymphomas that formed in NAC-treated animals displayed significantly less TUNEL-positive apoptotic cells compared with untreated controls ($P = .024$; data not shown). This difference was even larger in cells isolated from *E μ -myc* transgenic mice at a preneoplastic stage ($P = .006$; Figure 5B). Notably, Myc-inducible high ARF levels remained unchanged in response to NAC (Figure S3B-D), suggesting that NAC action attenuates an oncogene-evoked DDR but not oncogenic signaling to ARF. Notably, NAC-treated mice ($n = 19$) developed lymphomas with latencies comparable with untreated controls (data not shown), presumably due to a neutralizing net effect of the lowered induction of the DDR-initiated proapoptotic machinery and, simultaneously, the lowered selective pressure against this machinery and a slight reduction in proliferation when NAC is present. Importantly, NAC-protected control lymphomas, although lacking basal activation of DDR components (to compare with non-NAC-treated control lymphomas, see Figure 3A), consistently retained a functional DDR that became apparent only after exposure to ADR in vitro (Figure 5C, compare with Figure 3B). Therefore, NAC treatment effectively reduces marks of endogenous DNA damage and attenuates DDR-initiated apoptosis in Myc-driven lymphomagenesis, thereby uncovering ROS as critical mediators of the Myc-provoked DDR that is subsequently selected against in manifest lymphomas.

Preserving a functional Atm-governed DDR determines superior treatment outcome

Given the impaired ADR-inducible checkpoint responses in *Atm*^{–/–} and DDR-compromised control lymphomas in vitro, we tested whether a functional DDR machinery at diagnosis may predict superior short-term and long-term outcome to various DNA-damaging anticancer therapies in vitro and in vivo. Firstly, freshly isolated control lymphoma cells belonging to the DDR⁺, the DDR[–], or the NAC-protected group as well as *Atm*^{–/–} and *p53*-null lymphomas (ie, *E μ -myc* lymphomas that formed in *p53*^{+/-} mice and lost the remaining *p53* wild-type allele⁴) were exposed to increasing doses of ADR in vitro, and viability was assessed after 19 hours. DDR⁺ control lymphomas—like lymphomas that formed under NAC—displayed excellent sensitivity to ADR (Figure 6A). In contrast, *Atm*^{–/–} lymphomas and DDR[–] control lymphomas exhibited profound drug resistance only surpassed by the drug-

insensitive *p53*-null lymphomas. Notably, the poor sensitivity of *Atm*^{–/–} lymphomas was not due to additional genomic alterations, because preneoplastic *Atm*^{–/–} B cells were equally insensitive to ADR (Figure S4A). To further assess short-term drug-induced apoptosis in lymphomas of the respective groups growing in their natural environment, lymph node sections from mice harboring transplanted lymphomas obtained 4 hours after systemic treatment with the anticancer agent CTX were subjected to TUNEL staining. Again, DDR⁺ control and NAC-protected control lymphomas produced massive apoptosis in situ following CTX, whereas

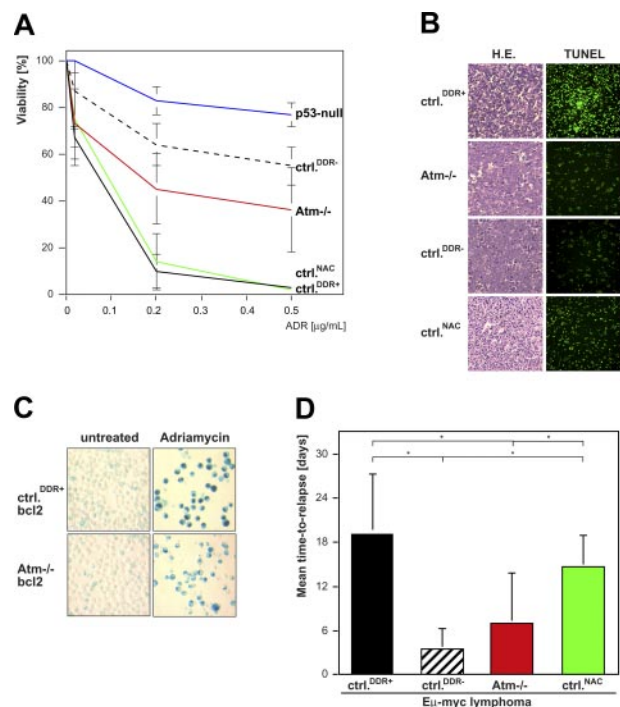


Figure 6. Preservation of an intact Atm-governed DDR determines treatment responses in vitro and in vivo. (A) 7-Amino-actinomycin D flow-based cytotoxicity analysis of the DDR⁺, DDR[–], and NAC-protected control lymphomas as well as *p53*-null and *Atm*^{–/–} lymphomas measured at 19 hours of ADR exposure at the indicated concentrations in vitro ($n = 3$ individual samples per group). (B) Cellular and nuclear apoptotic morphology by hematoxylin and eosin staining (H.E., left) and visualization of apoptotic DNA strand breaks by the TUNEL reaction (right) in lymphoma sections of the indicated groups 4 hours after intraperitoneal administration of 300 mg/kg CTX. (C) Representative cytospin preparations of Bcl2-expressing DDR-competent versus *Atm*^{–/–} lymphoma cells exposed to ADR for 7 days or left untreated and stained for senescence-associated β -galactosidase activity. Original magnification $\times 200$. (D) Time-to-relapse analysis of mice harboring lymphomas of the indicated groups after exposure to a single dose to a 4 Gy total body γ -irradiation (DDR-competent control lymphomas [ctrl^{DDR+}], $n = 7$; DDR-compromised control lymphomas [ctrl^{DDR–}], $n = 6$; *Atm*^{–/–} lymphomas, $n = 11$; NAC-protected control lymphomas [ctrl^{NAC}], $n = 8$). All quantitative data are mean \pm SD; * $P < .05$.

apoptosis was much more sparse in CTX-treated *Atm*^{-/-} and DDR⁻ control lymphomas (Figure 6B).

Recent reports on cellular senescence imposed as another tumor-suppressive DDR to oncogenic signals in early (pre)malignant lesions suggested that DDR defects may be selected for to overcome this barrier.^{5,9,10,14,51,54,55} Moreover, disruption of the senescence program might impact on treatment outcome as well, because drug-inducible senescence was shown to extend survival of mice harboring Myc lymphomas.³⁹ Therefore, we tested whether drug-inducible senescence remains available in the absence of *Atm*. Contrasting the premature senescent phenotype of *Atm*^{-/-} MEFs,⁵² Myc-driven *Atm*^{-/-} lymphomas, like controls, apparently form by either never imposing or bypassing oncogene-provoked senescence. However, both DDR⁺ control and *Atm*^{-/-} lymphoma cells, infected with *Bcl2* to protect from apoptosis, entered cellular senescence 7 days after exposure to ADR in vitro as demonstrated by senescence-associated β -galactosidase staining (Figure 6C). Hence, disruption of the DDR by spontaneous defects or loss of *Atm* genes compromises chemotherapy-inducible apoptosis while leaving cellular senescence as a drug-responsive program available.

Finally, we asked whether these differences in apoptotic short-term responsiveness would translate into different long-term outcome in vivo. To this end, mice harboring transplanted primary lymphomas received a single 4 Gy dose of total body γ -irradiation when lymph node enlargements became palpable. Using this well-tolerated dose, most animals entered a remission but all eventually relapsed. Mice harboring DDR⁺ control lymphomas achieved the most durable remissions, whereas those bearing DDR⁻ lymphomas displayed the shortest benefit from treatment (Figure 6D). The mean time to relapse in the *Atm*^{-/-} lymphoma group was significantly shorter compared with the DDR⁺ ($P = .004$) but not to the DDR⁻ control lymphoma group. The group of mice harboring NAC-protected lymphomas behaved similarly to the DDR⁺ control lymphoma group and responded significantly better when compared with the DDR⁻ control lymphoma group ($P < .001$). Hence, preservation of an intact DDR at diagnosis is critical for the execution of an apoptotic response and long-term outcome after DNA-damaging therapy in vivo.

Discussion

Our study is the first comprehensive genetic approach that mechanistically links oncogene-provoked DDR defects to treatment outcome in aggressive lymphomas in vivo. Using a well-established Myc-driven mouse model for the generation of primary lymphomas with defined genetic lesions that recapitulate genetic and histopathological features of human non-Hodgkin lymphomas,⁵³ we identified the 2-step DDR induction by ROS initiation followed by *Atm* transduction as the critical anticancer restraint that complements the ARF axis in response to Myc signaling. While in nononcogene-driven scenarios the precise impact of *Atm* inactivation on cell growth and death remained controversial,²⁷ the collaboration of *Atm* defects with oncogenic Myc action unmasks apoptosis as the key *Atm*-mediated effector mechanism in response to Myc. Importantly, our data not only demonstrated a significant acceleration of Myc-driven lymphomagenesis in an *Atm*^{-/-} background but unveiled, as a proof of relevance, spontaneous selection against a functional DDR during lymphoma formation, and this group indeed displayed a tendency

toward shortened tumor latencies (mean onset, 90 days for DDR⁻ versus 120 for DDR⁺ lymphomas).

We considered—in addition to ROS—other mechanisms by which oncogenes might activate the DDR machinery. Stalled DNA replication forks due to Myc-induced hyperproliferation may produce DNA damage that triggers an Atr/Nbs1/Chk1-governed checkpoint.⁵⁶⁻⁵⁸ Indeed, the increased amounts of Atr-P-S431 detected in Myc-driven lymphomas were suggestive for hyperreplication stress. Conversely, the slight decrease of proliferation in NAC-treated lymphomas might have been sufficient to no longer produce aberrant DNA replication intermediates, thereby canceling a key trigger of the Atr-mediated DDR checkpoint. However, evidence presented here argues for ROS as the critical oncogene-evoked initiator of proapoptotic DNA damage signaling. Firstly, enforced proliferation by LPS in primary nontransgenic B cells to a level reminiscent of mitogenic, constitutive Myc signaling failed to generate a profound increase in ROS and did not enhance γ -H2AX marks of DNA damage, thereby suggesting that Myc-evoked ROS and Myc-driven proliferation are largely independent effector functions. Secondly, acute induction of Myc in fibroblasts (ie, before a relevant impact on proliferation could have been observed) resulted in a DDR that was dependent on ROS, as demonstrated pharmacologically, and on *Atm*, as confirmed genetically. Thirdly, *E μ -myc* transgenic preneoplastic B cells (ie, prior to the potential acquisition of more complex genomic alterations during transformation) already displayed activated DDR components associated with cleavage of caspase-3, and this proapoptotic signature was entirely absent in the *Atm*-deficient counterpart despite Atr activation at this time (data not shown). In accordance with Atr's ability to substitute for *Atm* with delayed kinetics, it is not surprising to detect higher activation of Atr in *Atm*^{-/-} lymphomas, but apparently not as a functionally relevant component of proapoptotic signaling.⁴⁹ Fourthly, biallelic deletion of *Atm* dramatically shortened tumor latencies in Myc-driven tumor models irrespective of the activity of the Atr kinase. Taken together, while constitutive Myc signaling, presumably via hyperreplication stress, is undoubtedly associated with Atr activation, our data support the view that ROS are the critical mediators of proapoptotic Myc-induced DNA damage sensed and transduced primarily by *Atm*.

Our data add to the intense scientific debate on relative tumor-suppressive contributions of ARF-mediated versus DNA damage-initiated signals as upstream components of p53. Myc-driven hyperproliferation imposes an ARF response via E2F transcription factors,⁵⁹ although other *Atm*-independent, possibly metabolic pathways might also be involved in ARF induction. Recently, ARF inactivation was shown to disrupt p53's tumor-suppressive function in response to chemically induced oncogenic stresses in vivo, but no DDR-defective genetic model such as the *Atm*^{-/-} mouse was included in this setting.⁶⁰ In the *E μ -myc* transgenic mouse, tumor onset was accelerated by defined genetic ablation of *Atm* through impairment of p53-mediated apoptosis. Although p53 protein levels remained very low in response to even drug-induced DNA damage due to lack of protein-stabilizing posttranslational modifications in the absence of *Atm*, p53 apparently was still susceptible to ARF-mediated oncogenic signals. This duality of oncogenic signaling to p53 turned out to be amenable to pharmacologic dissection, because antioxidative intervention ablated the oncogene-evoked DDR without affecting Myc-mediated ARF induction in fibroblasts and B cells. As a consequence, neither *Atm* loss nor NAC treatment alleviated the pressure to inactivate components of the ARF/p53 axis in primary lymphomas. Thus, our data support the view that ROS on one side and oncogenic

hyperreplication on the other side challenge cellular countermeasures whose tumor-suppressive potential is rather complementary than overlapping. Accordingly, human tumors—and lymphoid malignancies in particular—not only frequently exhibit *INK4a/ARF* mutations but may present with simultaneous defects in the DDR machinery, namely at the level of the *Atm* kinase.^{61,62}

Whether selective defects in certain tumor suppressors or increased genetic instability may ultimately drive tumor development and progression remains an issue of debate. In our *Eμ-myc* model, compromised apoptosis as a consequence of *Atm* loss became already apparent in preneoplastic *Atm*^{-/-} B cells, but this defect did not permit the survival of cytogenetically grossly aberrant lymphomas; we rather observed lymphomas with close to normal chromosome counts harboring translocations indicative of improper DNA double-strand break repair in the absence of *Atm*. Likewise, nontransgenic *Atm*^{-/-} mice develop T-cell lymphomas that select for specific chromosomal alterations (for example, gains that include the *c-myc* locus) instead of randomly accumulating genomic aberrations.³¹ Hence, genetic instability may occur as a byproduct of *Atm* dysfunction, but *Myc*-driven lymphoma formation relies on sufficient suppression of latent proapoptotic capabilities by targeting both the *Atm/p53* and *ARF/p53* cascades.

Oncogene-derived ROS have important implications for the outcome of anticancer therapy, because their excessive presence may primarily activate but ultimately select against an intact proapoptotic DDR machinery at diagnosis or later during tumor progression (Figure 3 and data not shown). Recently, a pharmacologic approach was proposed to preferentially kill cancer cells by taking advantage of their abnormal ROS levels,⁶³ which might be of particular relevance to target tumors that failed to maintain an intact DDR-mediated death program. Despite the notion that anticancer agents such as ADR may function at least in part in some cell types via producing ROS,⁶⁴ DDR-protective application of NAC during tumorigenesis did not abrogate lymphoma susceptibil-

ity to the cytotoxic activity of various DNA-damaging treatment modalities in vivo (Figure 6), and NAC cotreatment did not reduce ADR-mediated cytotoxicity in vitro (Figure S5). Given the profoundly improved outcome of chemotherapy after exposure to the ROS scavenger during lymphomagenesis, it will be of particular clinical interest to test whether application of an antioxidant after tumor diagnosis or at even more advanced stages might help to maintain sensitivity to DNA-damaging anticancer therapy.

Acknowledgments

This work was supported by grants from the European Union and the Bundesministerium für Bildung und Forschung (B.S.) and the Deutsche Forschungsgemeinschaft and Deutsche Krebshilfe (C.A.S.).

We thank C. Barlow, M. Digweed, A. Harris, T. Jacks, and C. Sherr for mice and genotyping protocols; M. Eilers for the *c-MycER^{TAM}* construct; S. Spieckermann for excellent technical assistance; and members of Prof Schmitt's lab for helpful discussions and editorial comments.

Authorship

Contribution: M.R. designed and performed research and analyzed data; C.L., I.S., B.T., and C.R. performed research and analyzed data; H.S., B.D., and B.S. contributed to the preparation of the manuscript; and C.A.S. designed research and wrote the paper.

Conflict-of-interest disclosure: The authors declare no competing financial interests.

Correspondence: Clemens A. Schmitt, Max-Delbrück-Center for Molecular Medicine and Charité–Humboldt University, Department of Hematology/Oncology, Augustenburger Platz 1, 13353 Berlin, Germany; e-mail: clemens.schmitt@charite.de.

References

1. Lowe SW, Cepero E, Evan G. Intrinsic tumour suppression. *Nature*. 2004;432:307-315.
2. Zindy F, Williams RT, Baudino TA, et al. Arf tumor suppressor promoter monitors latent oncogenic signals in vivo. *Proc Natl Acad Sci U S A*. 2003; 100:15930-15935.
3. Eischen CM, Weber JD, Roussel MF, Sherr CJ, Cleveland JL. Disruption of the ARF-Mdm2-p53 tumor suppressor pathway in Myc-induced lymphomagenesis. *Genes Dev*. 1999;13:2658-2669.
4. Schmitt CA, McCurrach ME, de Stanchina E, Wallace-Brodeur RR, Lowe SW. *INK4a/ARF* mutations accelerate lymphomagenesis and promote chemoresistance by disabling p53. *Genes Dev*. 1999;13:2670-2677.
5. Braig M, Lee S, Loddenkemper C, et al. Oncogene-induced senescence as an initial barrier in lymphoma development. *Nature*. 2005;436:660-665.
6. Kamijo T, van de Kamp E, Chong MJ, et al. Loss of the ARF tumor suppressor reverses premature replicative arrest but not radiation hypersensitivity arising from disabled *atm* function. *Cancer Res*. 1999;59:2464-2469.
7. Bartkova J, Horejsi Z, Koed K, et al. DNA damage response as a candidate anti-cancer barrier in early human tumorigenesis. *Nature*. 2005;434: 864-870.
8. Gorgoulis VG, Vassiliou LV, Karakaidos P, et al. Activation of the DNA damage checkpoint and genomic instability in human precancerous lesions. *Nature*. 2005;434:907-913.
9. Bartkova J, Rezaei N, Liontos M, et al. Oncogene-induced senescence is part of the tumorigenesis barrier imposed by DNA damage checkpoints. *Nature*. 2006;444:633-637.
10. Mallette FA, Gaumont-Leclerc MF, Ferbeyre G. The DNA damage signaling pathway is a critical mediator of oncogene-induced senescence. *Genes Dev*. 2007;21:43-48.
11. Lee AC, Fenster BE, Ito H, et al. Ras proteins induce senescence by altering the intracellular levels of reactive oxygen species. *J Biol Chem*. 1999;274:7936-7940.
12. Vafa O, Wade M, Kern S, et al. *c-Myc* can induce DNA damage, increase reactive oxygen species, and mitigate p53 function: a mechanism for oncogene-induced genetic instability. *Mol Cell*. 2002;9: 1031-1044.
13. Tanaka S, Diffley JF. Deregulated G1-cyclin expression induces genomic instability by preventing efficient pre-RC formation. *Genes Dev*. 2002; 16:2639-2649.
14. Di Micco R, Fumagalli M, Cicalese A, et al. Oncogene-induced senescence is a DNA damage response triggered by DNA hyper-replication. *Nature*. 2006;444:638-642.
15. Savitsky K, Bar-Shira A, Gilad S, et al. A single ataxia telangiectasia gene with a product similar to PI-3 kinase. *Science*. 1995;268:1749-1753.
16. Varon R, Vissinga C, Platzner M, et al. Nibrin, a novel DNA double-strand break repair protein, is mutated in Nijmegen breakage syndrome. *Cell*. 1998;93:467-476.
17. Malkin D, Li FP, Strong LC, et al. Germ line p53 mutations in a familial syndrome of breast cancer, sarcomas, and other neoplasms. *Science*. 1990; 250:1233-1238.
18. Bell DW, Varley JM, Szydio TE, et al. Heterozygous germ line hCHK2 mutations in Li-Fraumeni syndrome. *Science*. 1999;286:2528-2531.
19. Chang EH, Pirollo KF, Zou ZQ, et al. Oncogenes in radioresistant, noncancerous skin fibroblasts from a cancer-prone family. *Science*. 1987;237: 1036-1039.
20. Shiloh Y. ATM and related protein kinases: safeguarding genome integrity. *Nat Rev Cancer*. 2003;3:155-168.
21. Bakkenist CJ, Kastan MB. DNA damage activates ATM through intermolecular autophosphorylation and dimer dissociation. *Nature*. 2003;421:499-506.
22. Pellegrini M, Celeste A, Difilippantonio S, et al. Autophosphorylation at serine 1987 is dispensable for murine *Atm* activation in vivo. *Nature*. 2006;443:222-225.
23. Ali A, Zhang J, Bao S, et al. Requirement of protein phosphatase 5 in DNA-damage-induced ATM activation. *Genes Dev*. 2004;18:249-254.
24. Lindstrom MS, Wiman KG. *Myc* and *E2F1* induce p53 through p14ARF-independent mechanisms in human fibroblasts. *Oncogene*. 2003;22:4993-5005.
25. Li Y, Wu D, Chen B, et al. ATM activity contributes to the tumor-suppressing functions of p14ARF. *Oncogene*. 2004;23:7355-7365.

26. Xu Y, Baltimore D. Dual roles of ATM in the cellular response to radiation and in cell growth control. *Genes Dev.* 1996;10:2401-2410.
27. Westphal CH, Rowan S, Schmaltz C, Elson A, Fisher DE, Leder P. atm and p53 cooperate in apoptosis and suppression of tumorigenesis, but not in resistance to acute radiation toxicity. *Nat Genet.* 1997;16:397-401.
28. Cuneo A, Bigoni R, Rigolin GM, et al. Acquired chromosome 11q deletion involving the ataxia telangiectasia locus in B-cell non-Hodgkin's lymphoma: correlation with clinicobiologic features. *J Clin Oncol.* 2000;18:2607-2614.
29. Haidar MA, Kantarjian H, Manshouri T, et al. ATM gene deletion in patients with adult acute lymphoblastic leukemia. *Cancer.* 2000;88:1057-1062.
30. Korz C, Pscherer A, Benner A, et al. Evidence for distinct pathomechanisms in B-cell chronic lymphocytic leukemia and mantle cell lymphoma by quantitative expression analysis of cell cycle and apoptosis-associated genes. *Blood.* 2002;99:4554-4561.
31. Liyanage M, Weaver Z, Barlow C, et al. Abnormal rearrangement within the alpha/delta T-cell receptor locus in lymphomas from Atm-deficient mice. *Blood.* 2000;96:1940-1946.
32. Pusapati RV, Rounbehler RJ, Hong S, et al. ATM promotes apoptosis and suppresses tumorigenesis in response to Myc. *Proc Natl Acad Sci U S A.* 2006;103:1446-1451.
33. Shreeram S, Hee WK, Demidov ON, et al. Regulation of ATM/p53-dependent suppression of myc-induced lymphomas by Wip1 phosphatase. *J Exp Med.* 2006;203:2793-2799.
34. Adams JM, Harris AW, Pinkert CA, et al. The c-myc oncogene driven by immunoglobulin enhancers induces lymphoid malignancy in transgenic mice. *Nature.* 1985;318:533-538.
35. Barlow C, Hirotsune S, Paylor R, et al. Atm-deficient mice: a paradigm of ataxia telangiectasia. *Cell.* 1996;86:159-171.
36. Jacks T, Fazeli A, Schmitt EM, Bronson RT, Goodell MA, Weinberg RA. Effects of an Rb mutation in the mouse. *Nature.* 1992;359:295-300.
37. Kamijo T, Zindy F, Roussel MF, et al. Tumor suppression at the mouse INK4a locus mediated by the alternative reading frame product p19ARF. *Cell.* 1997;91:649-659.
38. Dumon-Jones V, Frappart PO, Tong WM, et al. Nbn heterozygosity renders mice susceptible to tumor formation and ionizing radiation-induced tumorigenesis. *Cancer Res.* 2003;63:7263-7269.
39. Schmitt CA, Fridman JS, Yang M, et al. A senescence program controlled by p53 and p16INK4a contributes to the outcome of cancer therapy. *Cell.* 2002;109:335-346.
40. Hartley JM, Spanswick VJ, Gander M, et al. Measurement of DNA cross-linking in patients on ifosfamide therapy using the single cell gel electrophoresis (comet) assay. *Clin Cancer Res.* 1999;5:507-512.
41. Ehlich A, Martin V, Muller W, Rajewsky K. Analysis of the B-cell progenitor compartment at the level of single cells. *Curr Biol.* 1994;4:573-583.
42. Kamijo T, Weber JD, Zambetti G, Zindy F, Roussel MF, Sherr CJ. Functional and physical interactions of the ARF tumor suppressor with p53 and Mdm2. *Proc Natl Acad Sci U S A.* 1998;95:8292-8297.
43. Zindy F, Eischen CM, Randle DH, et al. Myc signaling via the ARF tumor suppressor regulates p53-dependent apoptosis and immortalization. *Genes Dev.* 1998;12:2424-2433.
44. Bertwistle D, Sherr CJ. Regulation of the Arf tumor suppressor in Emicro-Myc transgenic mice: longitudinal study of Myc-induced lymphomagenesis. *Blood.* 2007;109:792-794.
45. Schmitt CA, Yang M, Fridman JS, Baranov E, Hoffman RM, Lowe SW. Dissecting p53 tumor suppressor functions in vivo. *Cancer Cell.* 2002;1:289-298.
46. Smith DP, Bath ML, Metcalf D, Harris AW, Cory S. MYC levels govern hematopoietic tumor type and latency in transgenic mice. *Blood.* 2006;108:653-661.
47. Falck J, Mailand N, Syljuasen RG, Bartek J, Lukas J. The ATM-Chk2-Cdc25A checkpoint pathway guards against radioresistant DNA synthesis. *Nature.* 2001;410:842-847.
48. Burma S, Chen BP, Murphy M, Kurimasa A, Chen DJ. ATM phosphorylates histone H2AX in response to DNA double-strand breaks. *J Biol Chem.* 2001;276:42462-42467.
49. Ward IM, Chen J. Histone H2AX is phosphorylated in an ATR-dependent manner in response to replicational stress. *J Biol Chem.* 2001;276:47759-47762.
50. Sagun KC, Carcamo JM, Golde DW. Antioxidants prevent oxidative DNA damage and cellular transformation elicited by the over-expression of c-MYC. *Mutat Res.* 2006;593:64-79.
51. Bartkova J, Bakkenist CJ, Rajpert-De Meyts E, et al. ATM activation in normal human tissues and testicular cancer. *Cell Cycle.* 2005;4:838-845.
52. Xu Y, Yang EM, Brugarolas J, Jacks T, Baltimore D. Involvement of p53 and p21 in cellular defects and tumorigenesis in Atm^{-/-} mice. *Mol Cell Biol.* 1998;18:4385-4390.
53. Schmitt CA, Wallace-Brodeur RR, Rosenthal CT, McCurrach ME, Lowe SW. DNA damage responses and chemosensitivity in the Eμ-myc mouse lymphoma model. *Cold Spring Harb Symp Quant Biol.* 2000;65:499-510.
54. Braig M, Schmitt CA. Oncogene-induced senescence: putting the brakes on tumor development. *Cancer Res.* 2006;66:2881-2884.
55. Serrano M, Lin AW, McCurrach ME, Beach D, Lowe SW. Oncogenic ras provokes premature cell senescence associated with accumulation of p53 and p16INK4a. *Cell.* 1997;88:593-602.
56. Brown EJ, Baltimore D. Essential and dispensable roles of ATR in cell cycle arrest and genome maintenance. *Genes Dev.* 2003;17:615-628.
57. Stiff T, Reis C, Alderton GK, Woodbine L, O'Driscoll M, Jeggo PA. Nbs1 is required for ATR-dependent phosphorylation events. *EMBO J.* 2005;24:199-208.
58. Ray S, Atkuri KR, Deb-Basu D, et al. MYC can induce DNA breaks in vivo and in vitro independent of reactive oxygen species. *Cancer Res.* 2006;66:6598-6605.
59. Aslanian A, Iaquinta PJ, Verona R, Lees JA. Repression of the Arf tumor suppressor by E2F3 is required for normal cell cycle kinetics. *Genes Dev.* 2004;18:1413-1422.
60. Efeyan A, Garcia-Cao I, Herranz D, Velasco-Miguel S, Serrano M. Tumour biology: policing of oncogene activity by p53. *Nature.* 2006;443:159.
61. Gronbaek K, Worm J, Ralfkiaer E, Ahrenkiel V, Hokland P, Goldberg P. ATM mutations are associated with inactivation of the ARF-TP53 tumor suppressor pathway in diffuse large B-cell lymphoma. *Blood.* 2002;100:1430-1437.
62. Tort F, Hernandez S, Bea S, et al. CHK2-decreased protein expression and infrequent genetic alterations mainly occur in aggressive types of non-Hodgkin lymphomas. *Blood.* 2002;100:4602-4608.
63. Trachootham D, Zhou Y, Zhang H, et al. Selective killing of oncogenically transformed cells through a ROS-mediated mechanism by beta-phenylethyl isothiocyanate. *Cancer Cell.* 2006;10:241-252.
64. Kurz EU, Douglas P, Lees-Miller SP. Doxorubicin activates ATM-dependent phosphorylation of multiple downstream targets in part through the generation of reactive oxygen species. *J Biol Chem.* 2004;279:53272-53281.